Gen. Physiol. Biophys. (2023), **42,** 521–529

doi: 10.4149/gpb_2023027

Polydatin inhibited TNF-α-induced apoptosis of skeletal muscle cells through AKT-mediated p38 MAPK and NF-κB pathways

Yongli Liu[1,*], Fang Xie[2,*], Changhuai Lu[2], Zongbo Zhou[1], Shudong Li[2], Jia Zhong[2], Qian Li[2] and Xianfang Shao[2]

[1] *Department of Orthopedics and Traumatology, Haikou Hospital of Traditional Chinese Medicine, Haikou, China*
[2] *Department of Orthopedics and Traumatology, Changde Hospital Affiliated to Hunan University of Traditional Chinese Medicine, Changde, China*

Abstract. Skeletal muscle atrophy severely impacts one's quality of life. The effects and mechanism of polydatin on skeletal muscle atrophy are unclear. This study investigated the effects and mechanism of polydatin on TNF-α-induced skeletal muscle cells. The skeletal muscle cell atrophy model was established by inducing C2C12 cells with TNF-α. Cell viability, IL-1β levels and cell apoptosis were assessed. The mRNA and protein expression levels of apoptosis-related proteins were measured. Meanwhile, the binding of polydatin to AKT was analyzed by molecular docking. TNF-α reduced cell fusion and viability while up-regulated IL-1β level and promoted cell apoptosis. TNF-α activated AKT, NF-κB, and p38 MAPK signaling pathways. Polydatin reversed these effects induced by TNF-α, with a low concentration being more effective. Polydatin was predicted to bind to GLY162, PHE161, GLU198, THR195 and GLU191 sites of AKT protein through van der Waals force and conventional hydrogen bonds. Overexpression of AKT led to increased phosphorylation levels of AKT, p38, and p65 proteins, as well as IL-1β levels and cell apoptosis. Polydatin inhibited TNF-α-induced apoptosis of C2C12 cells by regulating NF-κB and p38 MAPK signaling pathways through AKT. This suggests that polydatin shows promise as a new drug for the treatment of skeletal muscle atrophy.

Key words: Polydatin — p38 MAPK — NF-κB — AKT

Abbreviations: ANOVA, analysis of variance; CCK8, Cell Counting Kit 8; DAB, diaminobenzidine; ELISA, Enzyme-Linked Immunosorbent Assay; POD, optical density peroxidase; RT-qPCR, reverse transcription-quantitative polymerase chain reaction; TNF-α, tumor necrosis factor-α.

Introduction

Skeletal muscle atrophy is a symptom of cachexia, which is associated with several chronic conditions including cancer, aging, diabetes, and heart failure (Wyart et al. 2022; Chiappalupi et al. 2020). Despite it is characterized by clear clinical signs, its underlying etiology remains complex and poorly understood. The elevated levels of pro-inflammatory, which

* These authors contributed equally to this work.
Correspondence to: Qian Li, Department of Orthopedics and Traumatology, Changde First Hospital of Traditional Chinese Medicine, No. 588 binhu Road, Wuling District, Changde 415000, China
E-mail: 13787862698@139.com
Xianfang Shao, Department of Orthopedics and Traumatology, Changde First Hospital of Traditional Chinese Medicine, No. 588 binhu Road, Wuling District, Changde 415000, China
E-mail: shaoxianfang2021@163.com

© The Authors 2023. This is an **open access** article under the terms of the Creative Commons Attribution-NonCommercial 4.0 International License (https://creativecommons.org/licenses/by-nc/4.0/), which permits non-commercial use, distribution, and reproduction in any medium, provided the original work is properly cited.

are prevalent in cachexia, suggest that the immune system has vital function in its genesis and progression (Webster et al. 2020). Among these cytokines, tumor necrosis factor-α (TNF-α) is particularly pertinent to this process (Patel and Patel 2017).

TNF-α is a pleiotropic cytokine that is released by activated macrophages and exerts different effects depending on the tissue it influences. It can impact cell proliferation and differentiation, inflammation, apoptosis and necrosis (Kalliolias and Ivashkiv 2016; Jang et al. 2021). In skeletal muscle, TNF-α induces apoptosis by triggering various signaling pathways, which eventually leads to skeletal muscle atrophy (Schakman et al. 2012; Gallo et al. 2015). This phenomenon has been observed in patients with chronic heart failure and low body mass index, as well as those with chronic obstructive pulmonary disease in their skeletal muscles (Adams et al. 1999; Agusti et al. 2002).

Various intracellular signaling pathways, including the AKT pathway, are involved in regulating skeletal muscle physiology and metabolism. Serine/threonine protein kinase known as AKT controls cell metabolism, proliferation, apoptosis and survival (Zhang X et al. 2011). When activated by various stimuli, AKT is phosphorylated and promotes cell survival by resisting the apoptotic pathway (Sun et al. 2018; Chen et al. 2021). Several studies have demonstrated the close association between AKT and the development of musculoskeletal disorders (Matheny et al. 2018; Jaiswal et al. 2019).

Polydatin, a polyphenolic monomer compound found in *polygonum cuspidatum*, a traditional Chinese medicine, modulates key signaling pathways in inflammation, oxidative stress and apoptosis (Fakhri et al. 2021; Karami et al. 2022). It has a wide range of therapeutic effects on cancer (Mele et al. 2019), cardiovascular disease (Ming et al. 2017), diabetes (Gong et al. 2017), neurodegenerative diseases (Lv et al. 2019), rheumatoid diseases (Masodsai et al. 2019), and skeletal diseases (Kang et al. 2020). However, little information is available regarding the pharmacological effects and regulatory mechanisms of polydatin on skeletal muscle atrophy.

In this work, we created a skeletal muscle atrophy cell model by treating C2C12 cells with TNF-α and investigated the impact of polydatin intervention on TNF-α-induced apoptosis, along with exploring the underlying mechanism. Ultimately, the study aimed to provide a theoretical basis for the clinical use of polydatin in the treatment of skeletal muscle atrophy.

Materials and Methods

Cell culture and treatment

C2C12 cells were originated from the Chinese Academy of Sciences (Shanghai, China) and cultured in DMEM (D5796, Sigma, USA) containing 10% FBS (10099141, Gibco, USA), 1% penicillin and 100 U/ml streptomycin (Beyotime, SV30010, China) in the condition of 37°C and 5% CO_2. Polydatin (P816149, ≥95%) was purchased from Shanghai Macklin Biochemical Technology Co., Ltd. Based on the previous research in Chinese, we treated C2C12 cells with different doses of polydatin (10, 25 and 50 mg/l) for 24 h, and the CCK8 method was used to test the cytotoxicity of polydatin on cells. *In vitro* skeletal muscle atrophy was simulated by treating C2C12 cells with TNF-α (10 ng/ml, Sigma, USA) for 24 h (Dun et al. 2015). Cells were grouped as follows: (1) Control group (PBS), (2) Model group (cells were treated with TNF-α for 24 h), (3) Polydatin-L group (cells were co-treated with TNF-α and 10 mg/l polydatin for 24 h), (4) Polydatin-M group (cells were co-treated with TNF-α and 25 mg/l polydatin for 24 h), (5) Polydatin-H group (cells were co-treated with TNF-α and 50 mg/l polydatin for 24 h). The viability and confluence of C2C12 cells were analysed and 10 mg/l was selected as the optimal concentration group of polydatin for subsequent experiments. C2C12 cells in logarithmic growth phase were then divided into four groups: (1) Model group (cells were treated with TNF-α for 24 h), (2) Polydatin group (cells were co-treated with TNF-α and 10 mg/l polydatin for 24 h), (3) Polydatin+oe-NC group (cells were transfected with empty plasmid for 48 h, then co-treated with TNF-α and 10 mg/l polydatin for 24 h), (4) Polydatin+oe-AKT group (cells were transfected with AKT overexpression plasmid for 48 h, then co-treated with TNF-α and 10 mg/l polydatin for 24 h).

Cell transfection

According to the manufacturer's instructions, cells were transfected with oe-AKT (HG-MO009652, HonorGene, China) using Lipofectamine 2000 (11668019, Invitrogen, USA) after they had achieved 70% confluence. The transfection process lasted for 48 h, with oe-NC serving as a control. After transfection, the cells were treated with TNF-α and polydatin.

Morphological observation

The cells in each treatment group were observed under an inverted biological microscopy (×100; DSZ2000X, Cnmicro, China) to assess their morphology, confluence, and number of viable cells.

Cell Counting Kit 8 (CCK8) assay

Trypsin digestion and counting of C2C12 cells were performed. Cells were seeded in 96-well plates at a concentration of 1×10^4 cells *per* well in a volume of 100 μl. Each group had three replicates. After the cells adhered to the plate surface, they were treated as described above. Upon completion of the assigned incubation time, the culture medium was aspirated from each well, and 10 μl of CCK-8 solution (NU679, DOJINDO), 10 μl of CCK-8 solution (NU679, DOJINDO, Japan) was introduced to each well. Thereafter, the samples were incubated for 2 h at 37°C. Finally, the absorbance (450 nm) was determined using a Bio-Tek microplate reader (MB-530, Heales, China).

Enzyme-Linked Immunosorbent Assay (ELISA)

IL-1β level in C2C12 cells supernatants was evaluated by IL-1β kit (CSB-E08054m, CUSABIO, China). A Bio-Tek microplate reader was used to evaluate the optical density (OD) at 450 nm.

TUNEL staining

The TUNEL apoptosis detection kit (40306ES50, YEASEN, China) was utilized to measure cell apoptosis based on the prescribed protocol. Paraffin sections were cleaned and permeabilized before being exposed to 50 μl TUNEL reaction mixtures in a moist box for 60 min at 37°C in the dark. After 30 min at 37°C in the presence of 50 μl of peroxidase, sections were cleaned with PBS to convert the signal. Subsequently, the sections were coated with 50 μl diaminobenzidine substrate solution and incubated there for 10 min at 25°C. Eventually, using a fluorescent microscope (BA410T, MOTIC, Singapore), apoptotic cells were observed.

Flow cytometry

To assess cell apoptosis, the FITC apoptosis kit (KGA1030, KeyGen, China) was served. Following treatment, trypsin-digested cells were gathered and then resuspended in 500 μl binding buffer, following a 5-min centrifugation at 2000 rpm. Subsequently, cells were then stained with 5 μl Annexin V-FITC and 5 μl Propidium Iodide in the absence of light for 15 min. It was conducted using a flow cytometer (A00-1-1102, Beckman, USA) to analyze the apoptotic cells.

Reverse transcription-quantitative polymerase chain reaction (RT-qPCR)

The manufacturer's instructions were followed while using the Trizol reagent (15596026, Thermo Fisher Scientific, USA) to extract the total RNA. Using the mRNA reverse transcription kit (CW2569, CWBIO, China), the extracted total RNA served as a template to reverse the cDNA. An UltraSYBR Mixture (CW2601, CWBIO, China), cDNA, and primer RT-qPCR system were used in the RT-qPCR (QuantStudio1, Thermo Fisher Scientific, USA). RT-qPCR was done three times as the following protocol: 2 min at 94°C, followed by 32 cycles (94°C for 30 s and 55°C for 45 s). GenePharma is where the primers were produced. $2^{-\Delta\Delta CT}$ was implemented to quantify the data. β-actin was applied for normalization. P38: forward, 5'-GACTTTGCCTCTACCTAGTGAACCC-3' and reverse 5'-TTTATTTCCCCTCGCAAGTCCT-3'. p65: forward, 5'-GATTCCCGATCTATCCAGTGAACCC-3' and reverse 5'-ATCCTTTUUUUTAGACAGTCCT-3'. AKT: forward, 5'-AGGGAGGTGTCATCTCAACTGA-3' and reverse 5'-CTCAACTGGTGTCGTGGAGTC-3'. β-actin: forward, 5'-ACCCTGAAGTACCCCATCGAG-3' and reverse 5'-AGCACAGCCTGGATAGCAAC-3'.

Western blotting

To extract the whole protein, RIPA buffer (P0013B, Beyotime, China) was performed. For protein quantification, a BCA kit was used. The protein (40 g *per* lane) was separated *via* 10% SDS-PAGE. The membranes were incubated overnight with primary antibodies. After then, proteins were introduced to PVDF membranes (Invitrogen, USA). Primary antibodies were added to the membranes and incubated with them overnight. The membranes were then blocked for 1 h with 5% skim milk. The primary antibodies used in this experiment include: anti-P38 (Proteintech; 14064-1-AP, 1:1000, USA), anti-p-P38 (Abcam; ab195049, 1:1000, UK), anti-Bcl-2 (Proteintech; 26593-1-AP, 1:500), anti-Bax (Proteintech; 50599-2-Ig, 1:5000), anti-caspase-3 (CST; #9661, 1:1000, USA), anti-p-p65 (Proteintech; 10088-1-AP, 1:500), anti-p65 (Proteintech; 18725-1-AP, 1:500), anti-AKT (Proteintech; 11306-1-AP, 1:5000), anti-p-AKT (Proteintech; 11306-1-AP, 1:5000) and anti-β-actin (Proteintech; 66009-1-Ig, 1:5000). The membranes were then coated with secondary antibodies (HRP-conjugated, Proteintech; SA00001-1, 1:5000) and incubated for 1 h. For the examination of protein bands, enhanced chemiluminescence (ECL) (Invitrogen, USA) was used. For data quantification, β-actin was adopted.

Molecular docking

The binding between polydatin and AKT was analysed using PubChem and PDB (https://www.rcsb.org/). In brief, the crystal compound formula of AKT with a resolution of less than 2.5 Å was obtained. The Autodock Vina software was used for molecular docking, and Hydrogen atoms that were added to the water molecules in AKT were deleted. Subsequently, the pro-protein ligands were extracted to generate a docking cavity. PyMol 2.4.0 was performed to visualize molecular docking results, and the stability of intermolecular binding between polydatin and AKT was reflected by observing the docking affinity score.

Statistical analysis

Each group underwent three separate experiments. GraphPad Prism 9.0 software was used to evaluate all data results, and the data were displayed as mean ± SD. Using Student's *t*-tests, the two groups were compared, and one-way analysis of variance (ANOVA) was performed to compare data from various sets. $p < 0.05$ suggested an obvious difference.

Results

Polydatin improved TNF-α-induced C2C12 cell injury

Firstly, we treated C2C12 cells with different concentrations (10, 25, and 50 mg/l) of polydatin to study its impact of polydatin on C2C12 cells. CCK8 data demonstrated that polydatin at concentrations of 10–50 mg/l increased the viability of C2C12 cells, with the most significant effect observed at a concentration of 10 mg/ml (Fig. 1B). Next, C2C12 cells were induced by 10 ng/ml TNF-α to establish a skeletal muscle atrophy model *in vitro*. As shown in Figure 1B, treatment with TNF-α resulted in a significant decrease in cell confluence and number, but co-treatment with polydatin partially eliminated these TNF-α-induced effects. Additionally, we found that TNF-α treatment decreased cell viability, and up-regulated the IL-1β level, both of which were reversed by polydatin, with the most significant effect observed at a concentration of 10 mg/l (Fig. 1C,D). Therefore, we chose to use 10 mg/l of polydatin for subsequent experiments. Taken together, our data indicated that polydatin might have a protective effect against TNF-α-induced damage in C2C12 cells.

Polydatin inhibited TNF-α-induced apoptosis of C2C12 cells

Then, we investigated the effects of polydatin on TNF-α-induced apoptosis of C2C12 cells. Flow cytometry analysis revealed that TNF-α treatment induced the apoptosis of C2C12 cells, while co-treatment with polydatin markedly reduced TNF-α-induced apoptosis (Fig. 2A). In addition, TNF-α treatment greatly upregulated the expression of Bax and cleaved caspase-3 and downregulated the expression of Bcl-2 in C2C12 cells, while these phenomena were abolished

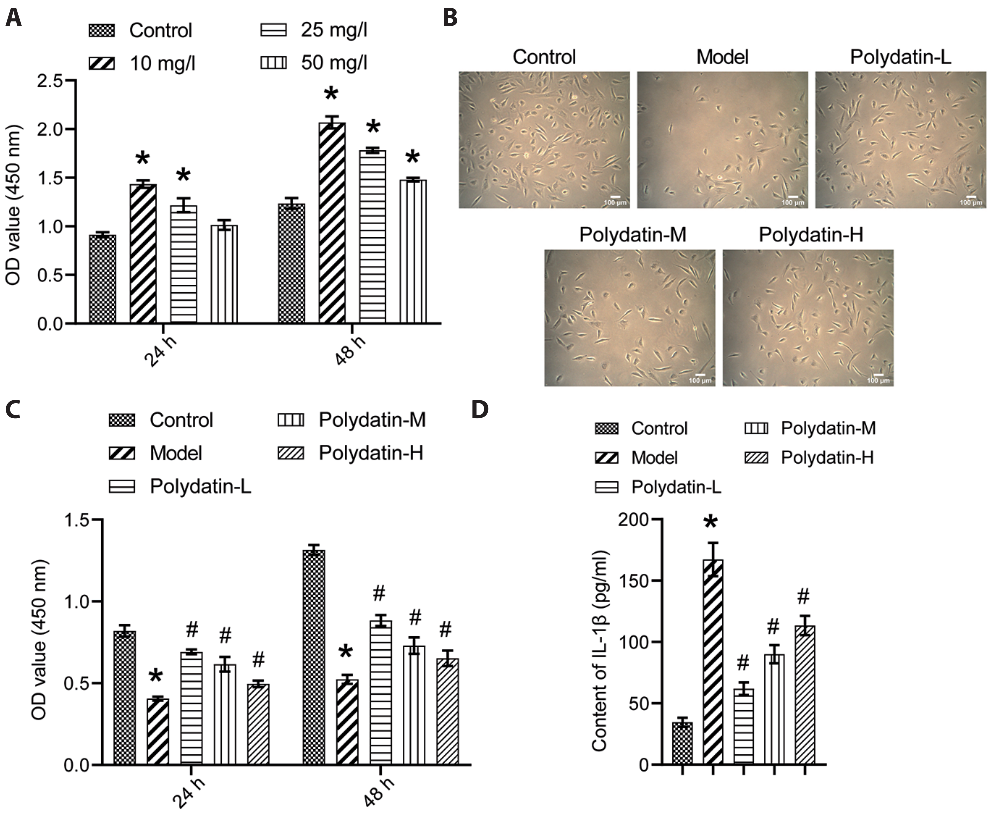

Figure 1. Polydatin improved TNF-α-induced C2C12 cell injury. C2C12 cells were exposed to polydatin for 24 or 48 h. **A**. CCK8 assay was conducted to determine the impact of varying concentrations (10, 25, and 50 mg/l) of polydatin on C2C12 cell viability. **B.** Microscopy was utilized to investigate the morphology of C2C12 cells when exposed to 10 ng/ml TNF-α and/or different concentrations (10, 25, and 50 mg/l) polydatin. Scale bar = 100 μm. **C.** The viability of C2C12 cells in different treatment groups was assessed by CCK8 assay. **D.** The contents of IL-1β in supernatants of C2C12 cells were examined by ELISA. * $p < 0.05$ compared to Control. # $p < 0.05$ compared to Model. Model, cells treated with TNF-α for 24 h; Polydatin-L, cells co-treated with TNF-α and 10 mg/l polydatin for 24 h; Polydatin-M, cells co-treated with TNF-α and 25 mg/l polydatin for 24 h; Polydatin-H, cells co-treated with TNF-α and 50 mg/l polydatin for 24 h.

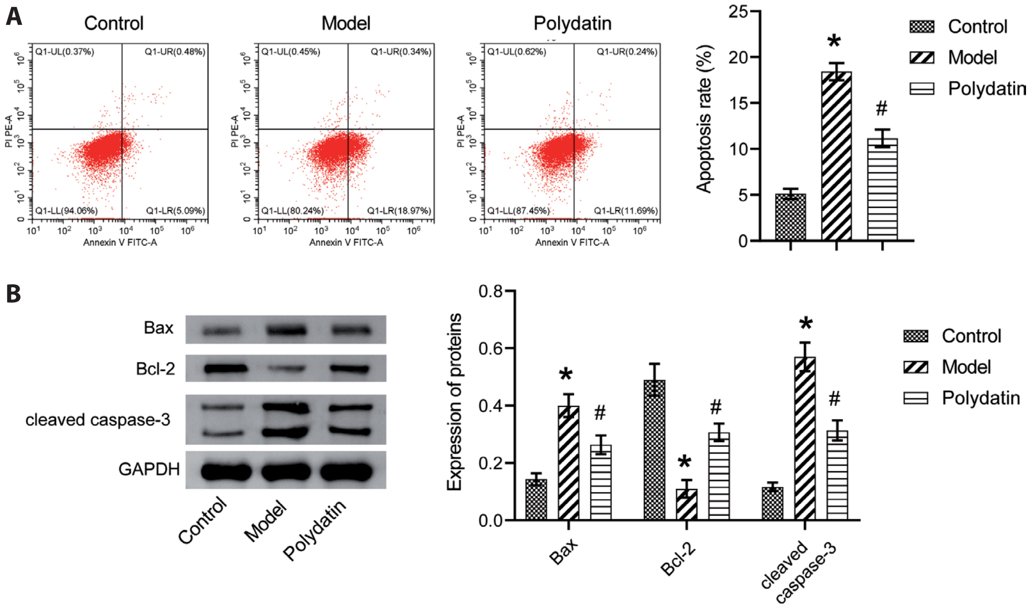

Figure 2. Polydatin inhibited TNF-α-induced apoptosis of C2C12 cells. **A.** Flow cytometry was used to detect the apoptosis of C2C12 cells exposed to 10 ng/ml TNF-α and/or 10 mg/l polydatin. **B.** The protein levels of Bax, Bcl-2 and cleaved caspase-3 in C2C12 cells treated with 10 ng/ml TNF-α and/or 10 mg/l polydatin were assessed by Western blot. * $p < 0.05$ compared to Control. $^{\#}$ $p < 0.05$ compared to Model.

by polydatin (Fig. 2B). Overall, our findings revealed that polydatin inhibited TNF-α-induced apoptosis of C2C12 cells.

Polydatin reversed TNF-α-induced activation of AKT, NF-κB and p38 MAPK signalings in C2C12 cells

To further study the mechanism of polydatin on TNF-α-induced C2C12 cells, we performed RT-qPCR and Western blot experiments. Our findings demonstrate that the mRNA expression of AKT, p38 and p65 were notably elevated in C2C12 cells following TNF-α treatment. However, treatment with polydatin nullified this TNF-α-induced effect, as illustrated in Figure 3A. Consistently, as demonstrated in Figure 3B, polydatin reversed the elevation in p38, p65 and AKT protein phosphorylation in C2C12 cells induced by TNF-α. To sum up, these results indicated that polydatin inhibited the TNF-α-induced activation of AKT, NF-κB and p38 MAPK signaling pathways in C2C12 cells.

Polydatin could bind to AKT

Subsequently, we utilized molecular docking to forecast the binding capacity of polydatin to AKT. As depicted in Figure 4A and B, polydatin might stably bind to GLY162, PHE161, GLU198, THR195 and GLU191 sites of AKT protein, which was mainly achieved by van der Waals force and conventional hydrogen bonds.

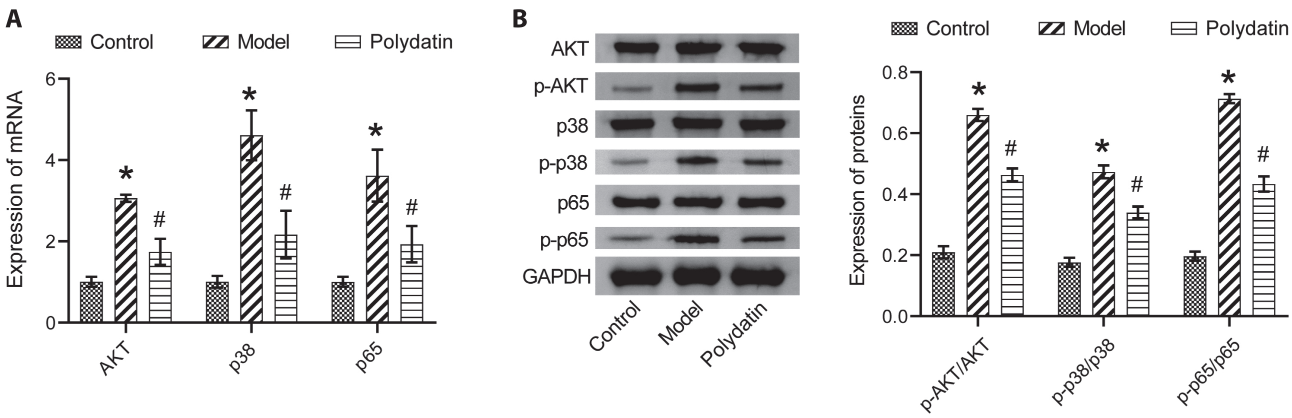

Figure 3. Polydatin reversed TNF-α-induced activation of AKT, NF-κB and MAPK/p38 signaling in C2C12 cells. **A.** The mRNA expression levels of AKT, p65 and p38 in C2C12 cells were detected by RT-qPCR. **B.** The phosphorylation levels of AKT, p38, and p65 proteins in C2C12 cells were examined by Western blot. * $p < 0.05$ compared to Control. $^{\#}$ $p < 0.05$ compared to Model.

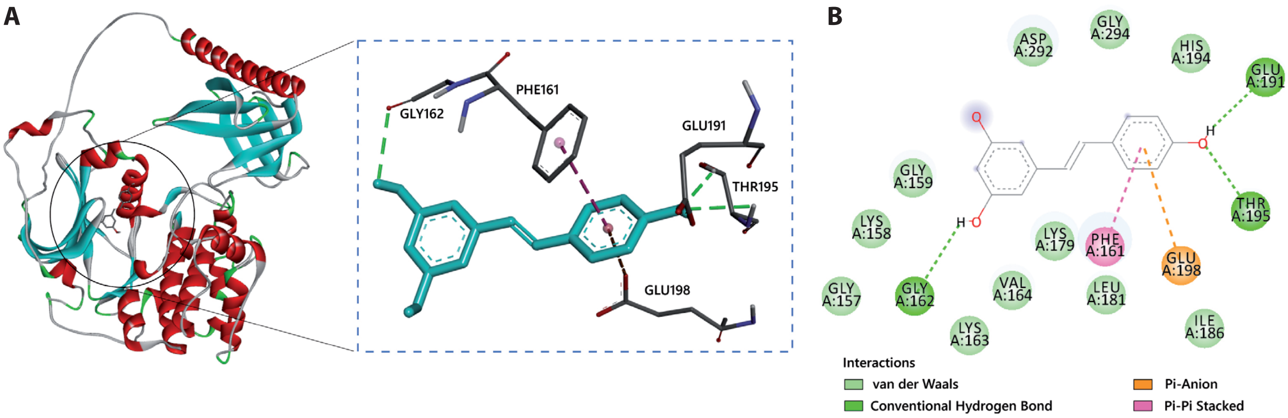

Figure 4. Polydatin could bind with AKT. Investigating the binding sites (**A**) and forces of interaction (**B**) between polydatin and AKT through molecular docking.

Overexpression of AKT reversed the effect of polydatin on TNF-α-treated C2C12 cells

Finally, AKT was overexpressed in C2C12 cells. As demonstrated in Figure 5A–C, polydatin downregulated the phosphorylation levels of AKT, p38, and p65 proteins and IL-1β levels in TNF-α-induced cells, and also suppressed apoptosis. However, these effects were countered by further overexpression of AKT. Taken together, overexpression of AKT reversed the effect of polydatin on TNF-α-treated C2C12 cells.

Discussion

Skeletal muscle atrophy can result from various factors, such as withdrawal (denervation, muscle unloading and fixation), hunger, aging, and multiple disease states (diabetes, cancer, AIDS) (Chiappalupi et al. 2020; Wyart et al. 2022). TNF-α induced apoptosis is a potential mechanism that leads to skeletal muscle atrophy (Schakman et al. 2012; Gallo et al. 2015). This study investigated the potential of polydatin in protecting skeletal muscle cells in a TNF-α-induced muscle atrophy model. The primary finding suggested that polydatin, through AKT-mediated p38 MAPK and NF-κB pathways, inhibited apoptosis in TNF-α-treated C2C12 cells, thereby preventing TNF-α-induced skeletal muscle atrophy.

TNF-α is a versatile cytokine with various effects, and its aberrant function is associated with several human diseases, such as cancer (Cruceriu et al. 2020) and Alzheimer's disease (Decourt et al. 2017). Polydatin, a polyphenolic monomer compound, has demonstrated therapeutic effects on various diseases. However, the pharmacological effects and regulatory mechanisms of polydatin on skeletal muscle atrophy have not been extensively explored. Our research discovered that polydatin at concentrations of 10–50 mg/l enhanced the viability of C2C12 cells, with the most significant impact being observed at low concentrations. When C2C12 cells were exposed to 10 ng/ml of TNF-α, the viability and confluence of the cells were significantly reduced, and the level of IL-1β was up-regulated. Nevertheless, polydatin was able to reverse the effects of TNF-α, with a significant effect observed at 10 mg/l. This result could be attributed to the activation of signaling pathways involved in cell growth and proliferation by polydatin. At lower concentrations, the drug may bind to target molecules, triggering cascade reactions and releasing factors that promote cell growth and proliferation, thereby enhancing cell viability. However, as the drug concentration increases, it may trigger negative feedback mechanisms or other antagonistic effects, inhibiting normal cell growth and proliferation. Furthermore, at high concentrations, the drug may induce cytotoxic effects leading to cell death. The specific mechanisms may involve the affinity and selectivity of the drug towards target molecules, as well as the modulation of relevant signaling pathways. However, further research and validation are required to precisely elucidate these mechanisms. Consequently, subsequent experiments utilized 10 mg/l of polydatin. Collectively, these results indicated that polydatin could improve TNF-α-induced C2C12 cell injury.

Apoptosis is a highly regulated cell suicide program that operates through finely controlled signaling pathways (Pistritto et al. 2016). In skeletal muscle, apoptosis exhibits unique characteristics due to the multinucleated nature of muscle cells. Specifically, the apoptosis-induced decay of a muscle nucleus does not result in "complete death" of muscle cells, but rather leads to the loss of gene expression within the local muscle nucleus domain, which can result in cell atrophy (Marzetti et al. 2012). Gallo et al. (2015) reported that TNF-α treatment increased apoptosis and NF-κB in C2C12 cells, and decreased AKT phosphorylation in C2C12 myotubes. Our study found that TNF-α treatment promoted the apoptosis of C2C12 cells, as evidenced by the increased expression of cleaved caspase 3 and Bax, and the decreased expression of Bcl-2. However, polydatin was seen to counteract these effects, indicating that polydatin could inhibit TNF-α-induced apoptosis of C2C12 cells.

Many studies have shown that activation of inflammatory cytokines and signaling pathways may be vital for inducing muscle atrophy (Doyle et al. 2011; Zhang G et al. 2011). AKT, a serine/threonine protein kinase, has been found to be closely related to the development of musculoskeletal (Matheny et al. 2018; Jaiswal et al. 2019). NF-κB is the main transcription factor induced by TNF-α, and its activation depends on the activity of AKT (Shang et al. 2019; Condorelli et al. 2002). Moreover, Lee et al. demonstrated that *Pyropia yezoensis* protein could inhibit the NF-κB pathway and antagonize the TNF-α-induced myotube atrophy (Lee et al. 2021). p38 MAPK has been recognized as a potential regulator of muscle catabolism, and targeting p38 MAPK may promote myogenesis and treat muscular dystrophy (Segalés et al. 2016; Brennan et al. 2021). Our study found that TNF-α significantly increased the mRNA and phosphorylation levels of AKT, p38 and p65 in C2C12 cells. However, treatment with polydatin inhibited these TNF-α induced effects. Molecular docking data showed that polydatin was predicted to bind to GLY162, PHE161, GLU198, THR195 and GLU191 sites of AKT protein, which was mainly achieved by van der Waals force and conventional hydrogen bonds. Furthermore, overexpression of AKT led to upregulation of phosphorylation levels

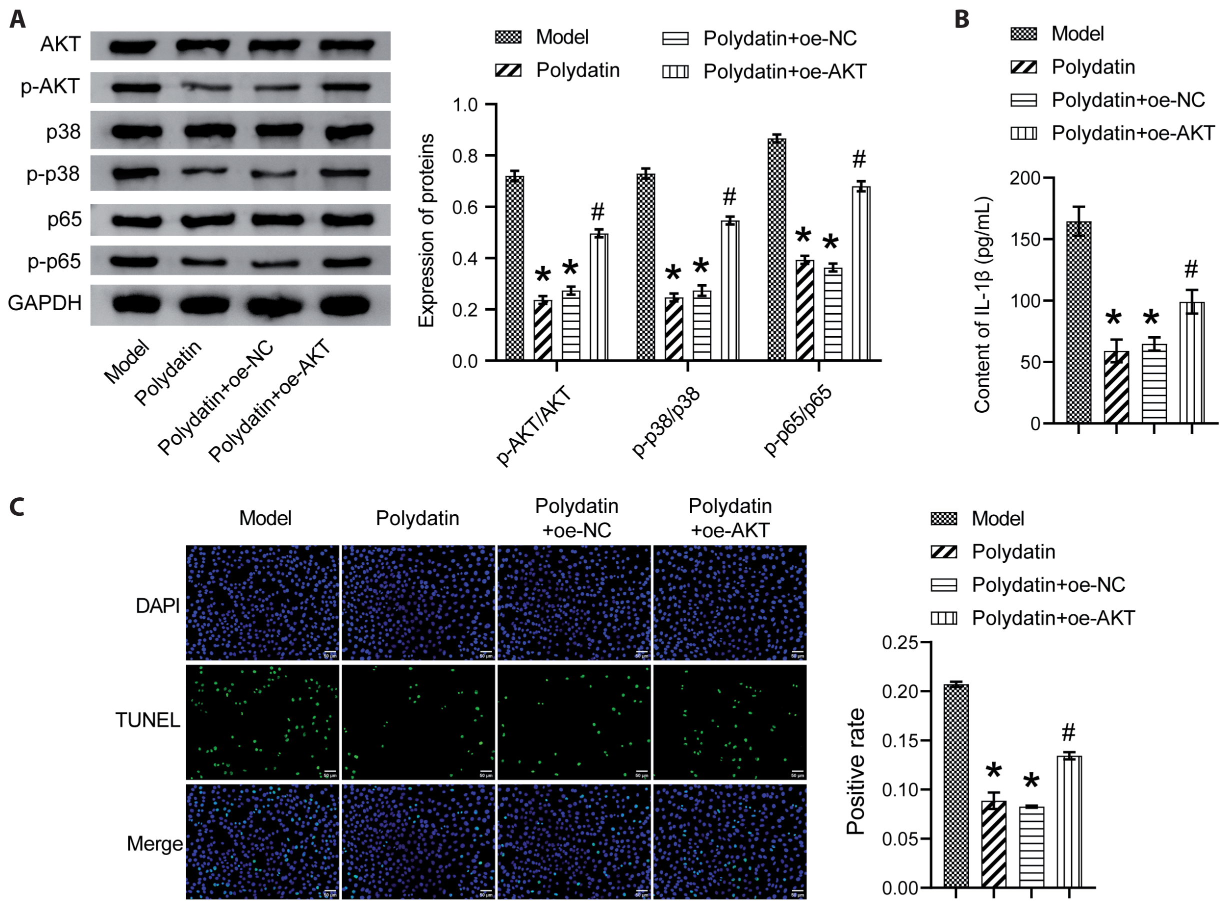

Figure 5. Overexpression of AKT reversed the inhibitory effect of polydatin on apoptosis of TNF-α-treated C2C12 cells. **A.** The phosphorylation levels of AKT, p38, and p65 proteins in C2C12 cells were examined by Western blot. **B.** The contents of IL-1β in supernatants of C2C12 cells were examined by ELISA. **C.** The apoptosis of C2C12 cells was assessed by TUNEL staining. Scale bar = 50 μm. * $p < 0.05$ compared to Control. # $p < 0.05$ compared to Model. Polydatin, cells co-treated with TNF-α and 10 mg/l polydatin for 24 h; Polydatin+oe-NC, cells were transfected with empty plasmid for 48 h, then co-treated with TNF-α and 10 mg/l polydatin for 24 h; Polydatin+oe-AKT, cells were transfected with AKT overexpression plasmid for 48 h, then co-treated with TNF-α and 10 mg/l polydatin for 24 h.

of AKT, p38, and p65 proteins, as well as IL-1β levels and promoted cell apoptosis.

In summary, polydatin inhibited the activation of p38 MAPK and NF-κB pathways by binding to AKT, thereby inhibiting TNF-α-induced apoptosis of C2C12 cells. Our study suggested that polydatin could serve as a promising lead compound for developing therapeutic drugs for TNF-α-induced skeletal muscle atrophy. However, *in vivo* studies are critical for identifying the pharmacological effects of polydatin in animal models.

Conflict of interest. The authors declare no conflict of interest.

Acknowledgements. This work was supported by the Key Project of Traditional Chinese Medicine research of Hunan Province (2020021) and the General project of Science and Technology Bureau of Changde city (2019S212).

References

Adams V, Jiang H, Yu J, Möbius-Winkler S, Fiehn E, Linke A, Weigl C, Schuler G, Hambrecht R (1999): Apoptosis in skeletal myocytes of patients with chronic heart failure is associated with exercise intolerance. J. Am. Coll. Cardiol. **33,** 959-965 https://doi.org/10.1016/S0735-1097(98)00626-3

Agustí AG, Sauleda J, Miralles C, Gomez C, Togores B, Sala E, Batle S, Busquets X (2002): Skeletal muscle apoptosis and weight loss in chronic obstructive pulmonary disease. Am. J. Respir. Crit. Care Med. **166,** 485-489 https://doi.org/10.1164/rccm.2108013

Brennan CM, Emerson CP Jr., Owens J, Christoforou N (2021): p38 MAPKs – roles in skeletal muscle physiology, disease mechanisms, and as potential therapeutic targets. JCI Insight **6,** e149915 https://doi.org/10.1172/jci.insight.149915

Chen K, Zhu P, Chen W, Luo K, Shi XJ, Zhai W (2021): Melatonin inhibits proliferation, migration, and invasion by inducing ROS-mediated apoptosis via suppression of the PI3K/Akt/mTOR signaling pathway in gallbladder cancer cells. Aging (Albany NY) **13,** 22502-22515 https://doi.org/10.18632/aging.203561

Chiappalupi S, Sorci G, Vukasinovic A, Salvadori L, Sagheddu R, Coletti D, Renga G, Romani L, Donato R, Riuzzi F (2020): Targeting RAGE prevents muscle wasting and prolongs survival in cancer cachexia. J. Cachexia Sarcopenia Muscle **11,** 929-946 https://doi.org/10.1002/jcsm.12561

Condorelli G, Morisco C, Latronico MV, Claudio PP, Dent P, Tsichlis P, Condorelli G, Frati G, Drusco A, Croce CM, et al. (2002): TNF-alpha signal transduction in rat neonatal cardiac myocytes: definition of pathways generating from the TNF-alpha receptor. FASEB J. **16,** 1732-1737 https://doi.org/10.1096/fj.02-0419com

Cruceriu D, Baldasici O, Balacescu O, Berindan-Neagoe I (2020): The dual role of tumor necrosis factor-alpha (TNF-α) in breast cancer: molecular insights and therapeutic approaches. Cell. Oncol. (Dordr.) **43,** 1-18 https://doi.org/10.1007/s13402-019-00489-1

Decourt B, Lahiri DK, Sabbagh MN (2017): Targeting tumor necrosis factor alpha for Alzheimer's disease. Curr. Alzheimer Res. **14,** 412-425 https://doi.org/10.2174/1567205013666160930110551

Doyle A, Zhang G, Abdel Fattah EA, Eissa NT, Li YP (2011): Toll-like receptor 4 mediates lipopolysaccharide-induced muscle catabolism via coordinate activation of ubiquitin-proteasome and autophagy-lysosome pathways. FASEB J. **25,** 99-110 https://doi.org/10.1096/fj.10-164152

Dun YL, Zhou XL, Guan HS, Yu GL, Li CX, Hu T, Zhao X, Cheng XL, He XX, Hao JJ (2015): Low molecular weight guluronate prevents TNF-alpha-induced oxidative damage and mitochondrial dysfunction in C2C12 skeletal muscle cells. Food Funct. **6,** 3056-3064 https://doi.org/10.1039/C5FO00533G

Fakhri S, Gravandi MM, Abdian S, Akkol EK, Farzaei MH, Sobarzo-Sánchez E (2021): The neuroprotective role of polydatin: Neuropharmacological mechanisms, molecular targets, therapeutic potentials, and clinical perspective. Molecules **26,** 5985 https://doi.org/10.3390/molecules26195985

Gallo D, Gesmundo I, Trovato L, Pera G, Gargantini E, Minetto MA, Ghigo E, Granata R (2015): GH-releasing hormone promotes survival and prevents TNF-α-induced apoptosis and atrophy in C2C12 myotubes. Endocrinology **156,** 3239-3252 https://doi.org/10.1210/EN.2015-1098

Gong W, Li J, Chen Z, Huang J, Chen Q, Cai W, Liu P, Huang H (2017): Polydatin promotes Nrf2-ARE anti-oxidative pathway through activating CKIP-1 to resist HG-induced up-regulation of FN and ICAM-1 in GMCs and diabetic mice kidneys. Free Radic. Biol. Med. **106,** 393-405 https://doi.org/10.1016/j.freeradbiomed.2017.03.003

Jaiswal N, Gavin MG, Quinn WJ 3rd, Luongo TS, Gelfer RG, Baur JA, Titchenell PM (2019): The role of skeletal muscle Akt in the regulation of muscle mass and glucose homeostasis. Mol. Metab. **28,** 1-13 https://doi.org/10.1016/j.molmet.2019.08.001

Jang DI, Lee AH, Shin HY, Song HR, Park JH, Kang TB, Lee SR, Yang SH (2021): The role of tumor necrosis factor alpha (TNF-α) in autoimmune disease and current TNF-α inhibitors in therapeutics. Int. J. Mol. Sci. **22,** 2719 https://doi.org/10.3390/ijms22052719

Kalliolias GD, Ivashkiv LB (2016): TNF biology, pathogenic mechanisms and emerging therapeutic strategies. Nat. Rev. Rheumatol. **12,** 49-62 https://doi.org/10.1038/nrrheum.2015.169

Kang L, Liu S, Li J, Tian Y, Xue Y, Liu X (2020): Parkin and Nrf2 prevent oxidative stress-induced apoptosis in intervertebral endplate chondrocytes via inducing mitophagy and anti-oxidant defenses. Life Sci. **243,** 117244 https://doi.org/10.1016/j.lfs.2019.117244

Karami A, Fakhri S, Kooshki L, Khan H (2022): Polydatin: Pharmacological mechanisms, therapeutic targets, biological activities, and health benefits. Molecules **27,** 6474 https://doi.org/10.3390/molecules27196474

Lee MK, Choi YH, Nam TJ (2021): Pyropia yezoensis protein protects against TNF-α-induced myotube atrophy in C2C12 myotubes via the NF-κB signaling pathway. Mol. Med. Rep. **24,** 486 https://doi.org/10.3892/mmr.2021.12125

Lv R, Du L, Zhang L, Zhang Z (2019): Polydatin attenuates spinal cord injury in rats by inhibiting oxidative stress and microglia apoptosis via Nrf2/HO-1 pathway. Life Sci. **217,** 119-127 https://doi.org/10.1016/j.lfs.2018.11.053

Marzetti E, Calvani R, Bernabei R, Leeuwenburgh C (2012): Apoptosis in skeletal myocytes: a potential target for interventions against sarcopenia and physical frailty – a mini-review. Gerontology **58,** 99-106 https://doi.org/10.1159/000330064

Masodsai K, Lin YY, Chaunchaiyakul R, Su CT, Lee SD, Yang AL (2019): Twelve-week protocatechuic acid administration improves insulin-induced and insulin-like growth factor-1-induced vasorelaxation and antioxidant activities in aging spontaneously hypertensive rats. Nutrients **11,** 699 https://doi.org/10.3390/nu11030699

Matheny RW Jr., Geddis AV, Abdalla MN, Leandry LA, Ford M, McClung HL, Pasiakos SM (2018): AKT2 is the predominant AKT isoform expressed in human skeletal muscle. Physiol. Rep. **6,** e13652 https://doi.org/10.14814/phy2.13652

Mele L, la Noce M, Paino F, Regad T, Wagner S, Liccardo D, Papaccio G, Lombardi A, Caraglia M, Tirino V, et al. (2019): Glucose-6-phosphate dehydrogenase blockade potentiates tyrosine kinase inhibitor effect on breast cancer cells through autophagy perturbation. J. Exp. Clin. Cancer Res. **38,** 160 https://doi.org/10.1186/s13046-019-1164-5

Ming D, Songyan L, Yawen C, Na Z, Jing M, Zhaowen X, Ye L, Wa D, Jie L (2017): trans-Polydatin protects the mouse heart against ischemia/reperfusion injury via inhibition of the renin-angiotensin system (RAS) and Rho kinase (ROCK) activity. Food Funct. **8,** 2309-2321 https://doi.org/10.1039/C6FO01842D

Patel HJ, Patel BM (2017): TNF-α and cancer cachexia: Molecular insights and clinical implications. Life Sci. **170,** 56-63 https://doi.org/10.1016/j.lfs.2016.11.033

Pistritto G, Trisciuoglio D, Ceci C, Garufi A, D'Orazi G (2016): Apoptosis as anticancer mechanism: function and dysfunction of its modulators and targeted therapeutic strategies. Aging (Albany NY) **8,** 603-619 https://doi.org/10.18632/aging.100934

Schakman O, Dehoux M, Bouchuari S, Delaere S, Lause P, Decroly N, Shoelson SE, Thissen JP (2012): Role of IGF-I and the TNFα/NF-κB pathway in the induction of muscle atrogenes by acute inflammation. Am. J. Physiol. Endocrinol. Metab. **303,** E729-739 https://doi.org/10.1152/ajpendo.00060.2012

Segalés J, Perdiguero E, Muñoz-Cánoves P (2016): Regulation of muscle stem cell functions: A focus on the p38 MAPK signaling pathway. Front. Cell. Dev. Biol. **4,** 91 https://doi.org/10.3389/fcell.2016.00091

Shang X, Lin K, Yu R, Zhu P, Zhang Y, Wang L, Xu J, Chen K (2019): Resveratrol protects the myocardium in sepsis by activating the phosphatidylinositol 3-kinases (PI3K)/AKT/mammalian target of rapamycin (mTOR) pathway and inhibiting the nuclear factor-κB (NF-κB) signaling pathway. Med. Sci. Monit. **25,** 9290-9298 https://doi.org/10.12659/MSM.918369

Sun J, Shi X, Li S, Piao F (2018): **2,**5-hexanedione induces bone marrow mesenchymal stem cell apoptosis via inhibition of Akt/Bad signal pathway. J. Cell. Biochem. **119,** 3732-3743 https://doi.org/10.1002/jcb.26602

Webster JM, Kempen L, Hardy RS, Langen RCJ (2020): Inflammation and skeletal muscle wasting during cachexia. Front. Physiol. **11,** 597675 https://doi.org/10.3389/fphys.2020.597675

Wyart E, Hsu MY, Sartori R, Mina E, Rausch V, Pierobon ES, Mezzanotte M, Pezzini C, Bindels LB, Lauria A, et al. (2022): Iron supplementation is sufficient to rescue skeletal muscle mass and function in cancer cachexia. EMBO Rep. 23 e53746 https://doi.org/10.15252/embr.202153746

Zhang G, Jin B, Li YP (2011): C/EBPβ mediates tumour-induced ubiquitin ligase atrogin1/MAFbx upregulation and muscle wasting. EMBO J. 30 4323-4335 https://doi.org/10.1038/emboj.2011.292

Zhang X, Tang N, Hadden TJ, Rishi AK (2011): Akt, FoxO and regulation of apoptosis. Biochim. Biophys. Acta **1813,** 1978-1986 https://doi.org/10.1016/j.bbamcr.2011.03.010

Received: March 3, 2023
Final version accepted: August 8, 2023